Linking the Chemical and Physical Effects of CO_2 Injection to Geophysical Parameters

Investigators:

Gary Mavko, Professor (Research), Tiziana Vanorio, Sr. Research Scientist, Geophysics; Sally Benson, Professor (Research) Energy Resources Engineering; Geophysics; Stephanie Vialle, Post-Doc, Geophysics, Stanford University. Andreas Luttge, Professor, Earth Science; Rolf Arvidson, Sr. Research Scientist, Earth Science, Rice University. Mrinal Sen, Professor, Corey Joy, Graduate Researcher, UT Austin

Abstract

This project aims to demonstrate techniques for quantitatively predicting the combined seismic signatures of CO_2 saturation, chemical changes to the rock frame, and pore pressure. This will be accomplished (i) by providing a better understanding the reaction kinetics of CO_2-bearing reactive fluids with rock-forming minerals, and (ii) by quantifying how the resulting long-term, CO_2-injection-induced changes to *the rock pore space and frame affect seismic parameters in the reservoir*. This research involves laboratory, theoretical, and computational tasks in the fields of both Rock Physics and Geochemistry. Ultrasonic P- and S-wave velocities are being measured over a range of confining pressures while injecting CO_2 and brine into the samples**.** Pore fluid pressure will be varied and monitored together with porosity during injection. The measurement of rock physics properties will be integrated and complemented by those obtained via geochemical experiments to link the physical and chemical processes underlying the mechanisms triggered by CO_2 injection.

In this report, we begin with a study aimed at better understanding how chemo-mechanical processes associated with CO_2 injection alter the pore-space attributes. The agreement between the evolution of velocity and permeability found in the laboratory and that expressed by the natural diagenetic trends shows that there are basic rules of pore space evolution dictated by the coupling between chemical and mechanical processes acting on a depositional-dependent microstructure. Carbonate facies determine the initial microstructure, which closely controls pore stiffness and the proneness to volumetric compaction during diagenesis. Depending on the effectiveness of compaction, changes in the rock may lead either to reduction in contact stiffness (high compaction) or connectivity enhancement (low compaction); eventually leading to two evolutionary patterns of velocity and permeability of carbonates experiencing underground circulation of aggressive fluids.

A second study was aimed at understanding the effects of injecting carbon dioxide rich brine on the elastic and transport properties of the Lower Tuscaloosa sandstone of Cranfield, Mississippi. We measured compressional and shear wave velocities

before and after injecting one sandstone sample with carbon dioxide rich synthetic Tuscaloosa brine at various confining pressures. The bulk and shear moduli decreased from 19 GPa and 12.4 GPa by roughly 9% and 6.5%, respectively, immediately following the first injection of 30 pore volumes of CO_2 rich synthetic Tuscaloosa brine. After injecting a total of 160 pore volumes, the rigidity remained constant and the bulk modulus decreased by a total of 13%, which is detectable on the seismic scale. The decrease in elastic properties is likely due to the dissolution of iron-bearing minerals and calcite that have formed at grain contacts as testified by the negligible change in porosity measured after injection. Decreasing the differential pressure acting on the core plug also decreased both P and S-wave velocities by 60 and 20 m/s respectively.

Introduction:

Monitoring, verification, and accounting (MVA) of CO_2 fate are three fundamental needs in geological sequestration. The primary objective of MVA protocols is to identify and quantify (1) the injected CO_2 stream within the injection/storage horizon and (2) any leakage of sequestered gas from the injection horizon, providing public assurance. Thus, the success of MVA protocols based on seismic prospecting depends on having robust methodologies for *detecting* the amount of change in the elastic rock property, *assessing* the *repeatability* of measured changes, and *interpreting and analyzing* the detected changes to make quantitative predictions of the movement, presence, and permanence of CO_2 storage, including leakage from the intended storage location. This project addresses the problem of how to interpret and analyze the detected seismic changes so that quantitative predictions of CO_2 movement and saturation can be made. The main goals are:

(a) linking the chemical and the physical changes occurring in the rock samples upon injection;
(b) assessing the type and magnitude of reductions caused by rock-fluid interactions at the grain/pore scale;
(c) providing the basis for CO_2-optimized physical-chemical models involving frame substitution schemes.

Background:

Having the appropriate rock-physics model is generally a key element for time-lapse seismic monitoring of the subsurface, both to infer the significance of detectable changes (*i.e.* qualitative interpretation) and to convert them into actual properties of the reservoir rocks (*i.e.* quantitative interpretation). Nevertheless, because of the peculiar ability of CO_2-rich water to promote physicochemical imbalances within the rock, we must address whether traditional rock-physics models can be used to invert the changes in geophysical measurements induced in porous reservoirs by the injection of CO_2, making it possible to ascribe such changes to the presence or upward migration of CO_2 plumes. Making this determination requires an understanding of the seismic response of CO_2-water-rock systems. Seismic reservoir monitoring has traditionally treated the changes in the reservoir rock as a physical-mechanical problem—that is, changes in seismic signatures are mostly modeled as

functions of saturation and stress variations (*e.g.* pore and overburden pressure) and/or intrinsic rock properties (*e.g.* mineralogy, clay content, cementation, diagenesis…). Specifically, modeling of fluid effects on seismic data has been based almost exclusively on Gassmann's equations, which describe the interaction of fluid compressibility with the elastic rock frame to determine the overall elastic behavior of rock. Beginning with the bulk (K_s) and shear (μ_s) moduli of the mineral composing the rock, we use Gassmann's fluid substitution scheme to compute the bulk modulus of the saturated rock (K_{sat}) from the bulk modulus of the fluid (K_{fl}) and from that of dry rock (K_{dry}). However, depending on the properties of the mineral composing the rock and the properties of the fluid, complex rock-fluid interactions may occur at the pore scale, leading to dissolution and formation of new mineralogical phases. All these physical modifications may compete in changing macroscopic rock properties such as permeability, porosity, and elastic velocities, which, in turn, can change the baseline properties for the Gassmann's fluid substitution scheme. This entails two consequences: (a) a classical fluid-substitution scheme may underpredict time-lapse changes and thus mislead 4D monitoring studies; and (b) predictions of *in situ* velocity will compensate for the chemically softened velocities with erroneous estimates of saturations and/or pore pressure.

Results

What Laboratory-ˇInduced Dissolution Trends Tell Us About Natural Diagenetic Trends of Carbonate Rocks. (Tiziana Vanorio, Yael Ebert, and Denys Grombacher, Stanford University, Submitted to joint Geological Society of London-AAPG Special Publication)

The pivotal idea of this study is to unfold the processes that control the heterogeneity in the attributes of the pore space in carbonates and, in turn, in the transport and elastic properties. Our objective is to investigate the mechanisms that may have been responsible for the pore space character. We use starting rocks of variable fabric –i.e., a depositional-dependent microstructure, induce a specific process – e.g., chemical dissolution under stress, then observe the development of the microstructure, permeability, porosity, and velocity due to the induced chemo-mechanical processes.

We find that the changes in the rock can lead to two different evolutionary trends of permeability and velocity, depending on the effectiveness of dissolution and compaction, which in turn depend on (a) the fraction of the carbonate phase characterized by high surface area and (b) the pore stiffness of the rock. Carbonates that compact significantly upon dissolution show a reduction in contact stiffness leading to a decrease in velocity and an increase in permeability. The latter is curbed by the ongoing compaction. Carbonates experiencing minimal or negligible compaction show a slight change in porosity and velocity; however large permeability changes are observed that are related to an enhancement in connectivity or decrease in the tortuosity of the pathways.

The fundamental argument driving this study is that the spatial distribution of carbonate reservoir properties is a product of interactions between 1) the specific diagenetic process acting upon the rock, 2) the parameters controlling fluid type and circulation (e.g., pH and flow rate) and 3) the original depositional facies defining the intrinsic mechanical response of the rock to chemical changes.

The key question is this: when we introduce a chemically reactive fluid in a carbonate rock under stress, how does the pore space change in response to stress redistribution and microstructure adjustment as the fluid-rock system attains a new chemo-mechanical equilibrium. Because unraveling continuous sequences of diagenetic events due to dissolution and compaction is difficult and ambiguous, we use a forward modeling approach: we directly monitor the evolution of porosity, permeability, compressional and shear velocities (PPV trends) of different depositional carbonate facies. Different facies imply a different texture, and in turn, a variable pore type and pore compressibility. We induce chemical dissolution by flooding the rock samples with a carbonic acid solution (~pH=3.5) while monitoring the mechanical deformation under stress and the induced changes in transport and elastic properties. In our experiments, we monitor the evolution of both transport and elastic parameters to 1) comprehensively look at what attribute of the pore space is more likely responsible for the changes, given the original texture of the rock, and 2) learn whether the induced modifications to the microstructure lead to systematic patterns in rock properties which are characteristic of specific carbonate facies.

We conduct several laboratory experiments to investigate and monitor the evolution of the pore network attributes responsible for variations in porosity, permeability, and P- and S-wave velocities of carbonate rocks. The experiments consist of flow-through injections of an aqueous CO_2 solution into samples under confining pressure. Injections are performed under variable confining pressure, while maintaining a nearly constant downstream flow rate of 5ml/min. Effective pressure is kept constant upon injection and ranges between 2 MPa and 5 MPa depending on the trade-off between sample permeability and flow rate. Several cumulative injections are performed during each experimental run. The main objective is to expose samples to increasing pore volumes of fluids and understand the role of the continued exposure on the trends of the measured properties. After each flooding, we characterize the samples' helium porosity, Klinkenberg-corrected nitrogen permeability, and ultrasonic P- and S-wave velocity. Time-lapse SEM imaging of the samples is performed after injection to relate changes in the physical properties to those in the rock microstructure. Helium gas is flowed at 150 psi through the sample after each injection for 8 hours to ensure drying within the vessel. This allows us to measure and monitor the variation of the properties of the frame alone while minimizing dispersion effects on velocity due to high frequency (Mavko and Jizba, 1991). During injection, the plugs are jacketed with rubber tubing to isolate them from the confining pressure medium. PZT-crystals mounted on steel endplates are used to generate P- and S-waves (1 MHz for P-waves and 0.7 MHz for S-waves). To monitor the rock strain driven by chemical dissolution under stress, we monitor a) the length decrease of the samples as a function of stress, which we then relate to porosity

loss upon compaction and b) the concentration of calcium in the output fluid, which we relate to porosity enhancement by dissolution. The total net change in porosity is thus the resulting porosity from each component. We estimate the accuracy in velocity, porosity and permeability measurements to be approximately ±1%, ±1%, and ±2%, respectively.

Figures 1a and 1b show the changes in bulk and shear moduli of the dry frame of a micritic grainstone/chalk (MA formation) upon injecting increasing volumes of the aqueous CO_2 solution. Moduli data are colored-coded as functions of confining pressure. Several important results are apparent in these data. First, as the first pore volumes are injected (14.3 Pv), both moduli (and by proxy velocities) decrease in magnitude (Figure 1a and Figure 1b), implying either an increase in porosity, a reduction in the stiffness at the grain contacts, or both. Second, the decrease in elastic moduli levels off over time despite continued injection of the acidic solution (Figure 1a and Figure 1b). Similarly, the amount of Ca++ measured from the effluent fluid at the outlet also levels off, implying a reduced rate of calcite dissolution (Figure 1d). Third, the decrease in velocity is pressure dependent.

Figure 1c shows how the P-wave velocity of the dry frame varies as a function of confining pressure; data are color-coded by number of injected pore volumes. For each pressure, the decrease in velocity with respect to its pre-injection value increases, while pressure decreases from 15MPa to 5MPa (Figure 1c). This translates into an increased sensitivity of velocity to pressure as injection proceeds, which implies a change in pore stiffness.

Figure 2 shows the porosity evolution of the rock sample as measured after each injection. At first, the sample experiences mechanical compaction due solely to the effect of confining pressure (Injected pore volume=0). Porosity progressively decreases from ~25.2% (black circle) to ~23.2% (blue diamonds at 15MPa) as pressure increases (Figure 2a). As injection proceeds, the sample experiences two competing mechanisms. On the one hand, dissolution of calcite leads porosity to increase (orange circles, Figure 2b). On the other hand, the sample experiences a concurrent, pressure-dependent compaction driven by dissolution (Figure 2a). Compaction is likely due to internal creeping under constant stress resulting from the decreased rock strength. Thus, the total net evolution in porosity of the sample upon dissolution under stress (Figure 2b) is the sum of both processes and is calculated by considering the change in porosity due to each component. Figure 2b also shows that porosity enhancement due to dissolution overwhelms the loss in porosity due to compaction, resulting in a net porosity increase after flooding.

Figure 3 shows the variations of elastic moduli, velocity, and Ca++ concentration upon injection through a tight limestone (MSA formation). Before injection, the tight limestone shows much lower velocity-pressure sensitivity than does the micritic grainstone (Figure 1c and Figure 3c - blue diamonds), implying a stiffer pore network. The different pressure sensitivity translates to a much smaller porosity loss in the limestone due to pressure dependent compaction (Figure 2a and Figure 4a –

data points at Pv equal to zero). After injection, there are three main differences between the tight limestone and the micritic grainstone. First, the magnitude of the decrease in elastic moduli (and by proxy velocity) of the tight limestone is smaller than that of the micrite-rich grainstone (Figure 1 and Figure 3). Also, the decrease does not level off as much as observed in the micrite-rich grainstones. Second, the tight limestone experiences less dissolution, as highlighted by the smaller concentration of Ca++ measured within the outlet fluid (Figure 1d and Figure 3d). This leads eventually to a smaller porosity enhancement from dissolution (Figure 2b and Figure 4b). Third, as the injected pore volumes increase, the tight limestone experiences less dissolution-induced compaction than does the micrite-rich grainstone (Figure 2a and Figure 4a). As a result, porosity enhancement due to dissolution does not strongly overwhelm the already minimal porosity loss due to compaction, resulting in a minimal porosity increase overall (Figure 4b). As do the grainstones, limestones show an increased sensitivity of velocity to pressure with flooding (Figure 3c), which is particularly visible at low pressures ranges.

In Figure 5, we compare the evolution of velocity and permeability of the treated samples to the natural diagenetic trends of untreated (not injected) carbonate samples (gray symbols). Data are plotted against porosity, and the different colors describe different injected samples; the black-circled symbol refers to the value measured for each sample before injection. Thus, the observed trends reflect how the modifications in the pore attributes and microstructure due to dissolution under stress affect velocity and permeability. Although the number of injected pore volumes is nearly the same for each sample, the evolution trends of properties vary across facies, with some similarities among samples belonging to the same facies/formation. In chalky, micritic carbonates (MA and high-porosity FP formations), both porosity and permeability increase upon injection, while velocities strongly decrease. In limestones (tight MSA and low-porosity FP formation), porosity and velocity show negligible change upon injection, while permeability greatly increases after reaching a critical threshold. Another noteworthy and surprising result is that the evolution of both velocity and permeability of the injected samples follows the natural diagenetic trends. Dissolution seems to primarily affect the permeability of tight limestones while leaving porosity and velocity essentially unaltered. Conversely, dissolution greatly affects the decrease in velocity of micrite-rich samples with a rate that increases going from grainstones to lime mudstones. For this facies, both permeability and porosity slightly increase as dissolution proceeds.

Transport and elastic properties depend on different attributes of the pore space. While stiffness at the grain contacts, porosity, and pore compliance control velocity (Anselmetti and Eberli 1993, Mavko et al. 2008, Weger et al. 2009), pore connectivity, tortuosity, and pore size control permeability (Carman 1961). Any change of these parameters during diagenesis defines the evolution of permeability, porosity and velocity. This paper shows that to understand their evolution, it is vital to couple dissolution, stress, and the original pore stiffness of the rock inherited by the depositional environment, which ultimately defines the microstructure of the rock. It is clear that the combination of the initial rock microstructure and the sequence of

events to which it is exposed enormously increases the number of possible deviations from first-order relationships between geophysical observables and rock properties (e.g., porosity and permeability).

Data comparison between micrite-rich grainstones and tight limestones show that the evolution of permeability and velocity in carbonates, due to leaching and/or more advanced dissolution, is microstructure-dependent. Under constant stress, carbonates experience dissolution-induced compaction (Figure 2 and Figure 4) as a result of the decreased strength of the rock. This weakening results exclusively from the removal of carbonate phases with high surface area (i.e., micrite and cement). Dissolution and compaction compete and feed back to each other. The results depend on (1) the specific pore-stiffness of the rock, which controls the amount of compaction, (2) the amount of micrite and/or cement, which is responsible for selective dissolution, and (3) the tightness of the formation, which, by defining permeability, influences the effective fluid circulation and the balance between dissolution and precipitation. Altogether, these factors determine how velocity and permeability of carbonates evolve under stress. In micrite-rich grainstones, pores that are more compliant than in tighter limestones, as well as the presence of high-surface-area phases (i.e., microcrystalline calcite), favor dissolution and dissolution-induced compaction. Dissolution of cement and micrite causes compaction as well as grain slip and rearrangement~~),~~ ultimately reducing the stiffness at the grain contacts. Therefore, injecting increasing volumes of fluid into a compacting sample does not lead to further decrease in the elastic moduli, which instead level off as injection proceeds. This is particularly important when monitoring injection of reactive fluids into carbonate reservoirs by time-lapse seismic. In addition, compaction continuously compensates for the enhancement in porosity and the enlargement of pore throats resulting from dissolution, hence curbing the increase of the permeability of these rocks. In tight limestones, the finely interlocked mosaic of micrite rhombohedra makes the deposition-inherited microstructure of these rocks very stiff (i.e., they have high pore stiffness). This, in turn, makes this rock type very insensitive to compaction. As a consequence, the enlargement of pore throats and microporosity due to dissolution is only minimally counteracted by the compaction. In addition, the relatively low permeability favors a poor dewatering of the Ca++ ion-rich water as well as supersaturation, which leads calcite to precipitate and weld micro-grains together under the effect of pressure. The direct consequence of these processes is that the enhancement of pore throats does not contribute much to the total porosity or to the decrease in velocity. However, it definitely affects pore connectivity (and likely tortuosity), leading the permeability of these tight microstructures to greatly increase.

One of the most important results of this study is that the evolution of both velocity and permeability of the injected samples follows the natural diagenetic trends of the facies. The similarities of the induced evolution of properties with those depicted by the natural diagenetic trends imply that pore attributes modify and the rock microstructure readjusts through common rules that are characteristic of each carbonate facies. Thus, the original depositional facies defines the intrinsic

mechanical response of the rock to chemical changes, playing a major role in the way pore space modifies under chemo-mechanical processes. These rules seem to create systematic patterns in rock properties, whose evolution is mainly controlled by compaction, and in turn, surface area and pore stiffness. Depending on the effectiveness of compaction, changes in the rock lead either to reduction in contact stiffness (high compaction) or connectivity enhancement (low compaction). These factors are key to future model-building strategies and/or pore-scale computation of processes aiming at property predictions in carbonate reservoir characterization.

By monitoring the evolution of porosity, permeability, and velocity upon dissolution-induced compaction, the results in this paper provide a better understanding of how chemo-mechanical processes alter the pore-space attributes. Since the experimental results mirror diagenetic trends, they also provide new insights to predict the evolution of the products of these alterations within the reservoir - i.e., porosity and permeability heterogeneity as well as acoustic response of laterally variant units. The agreement between the evolution of velocity and permeability found in the laboratory and that expressed by the natural diagenetic trends of the facies simply shows that there are basic rules controlling the way pore attributes modify upon diagenesis, rules which are dictated by the coupling between chemical and mechanical processes acting on a depositional dependent microstructure. This synergy defines how pore-space parameters change, creating the scatter in the velocity and permeability data in carbonates. Carbonate facies determine the initial microstructure, which closely controls pore stiffness and the proneness to volumetric compaction during diagenesis. Depending on the effectiveness of compaction, changes in the rock may lead either to reduction in contact stiffness (high compaction) or connectivity enhancement (low compaction); eventually leading to two evolutionary patterns of velocity and permeability of carbonates experiencing underground circulation of aggressive fluids.

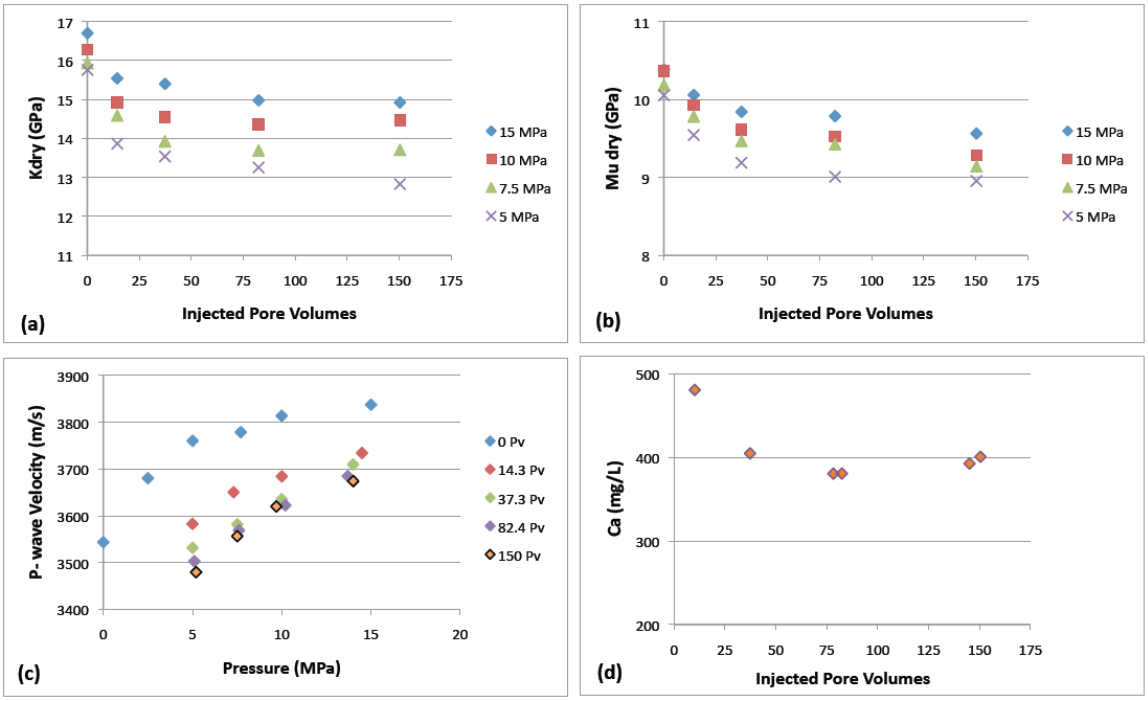

Figure 1: Variation of the bulk (a) and shear (b) moduli as functions of injected pore volumes. Data refer to micrite-rich grainstone from the MA formation and are color-coded as a function of confining pressure, (c) variation of P-wave velocity as a function of confining pressure. Data are color-coded as a function of the injected pore volumes, (d) variation of the concentration of the ion calcium in the collected fluid as function of the injected pore volumes.

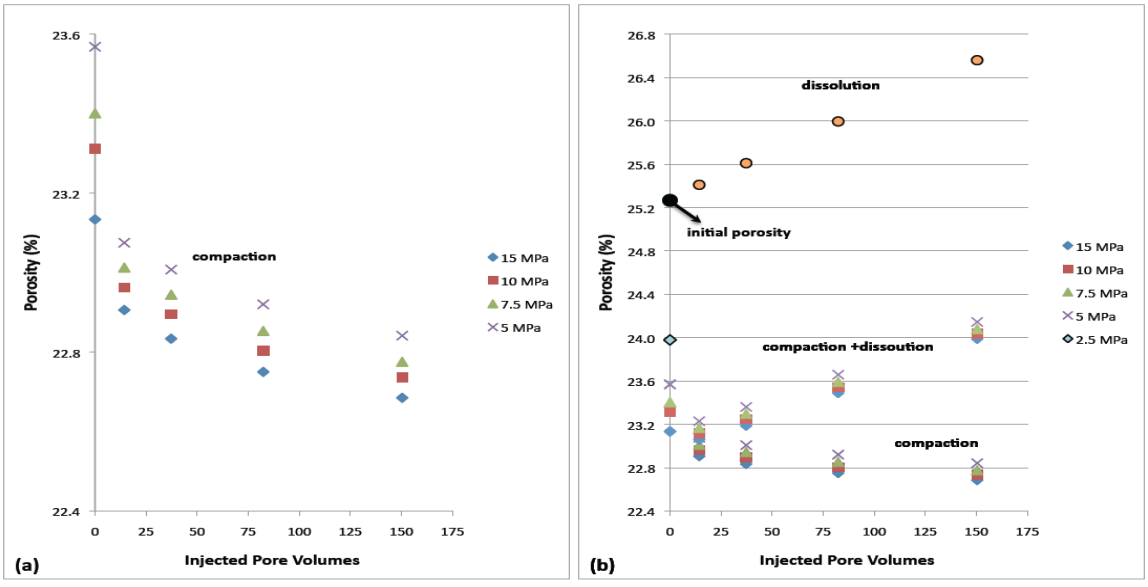

Figure 2: Variation of the porosity of the MA micrite-rich grainstone as a function of the injected pore volumes. The sample experiences a dissolution-driven compaction under the effect of the applied stress, eventually leading to porosity change.

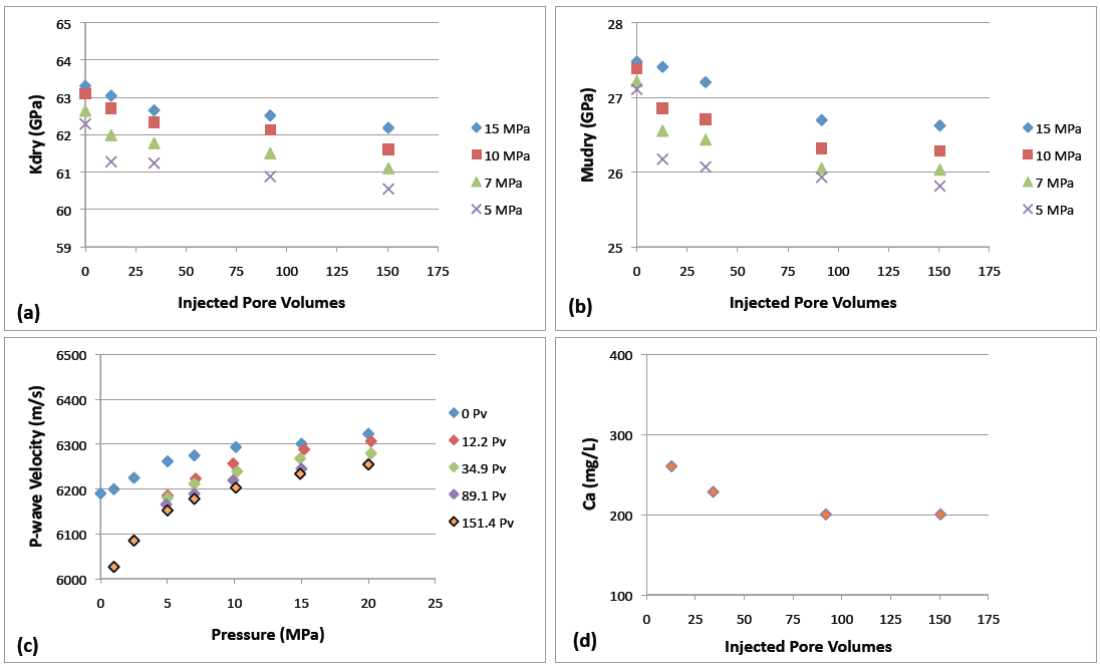

Figure 3: Variation of the bulk (a) and shear (b) moduli as functions of injected pore volumes. Data refer to a tight limestone from the MSA formation and are color-coded as functions of confining pressure, (c) variations of P-wave velocity as a function of confining pressure. Data are color-coded as functions of the injected pore volumes, (d) variation of the concentration of the ion calcium in the collected fluid as a function of the injected pore volumes.

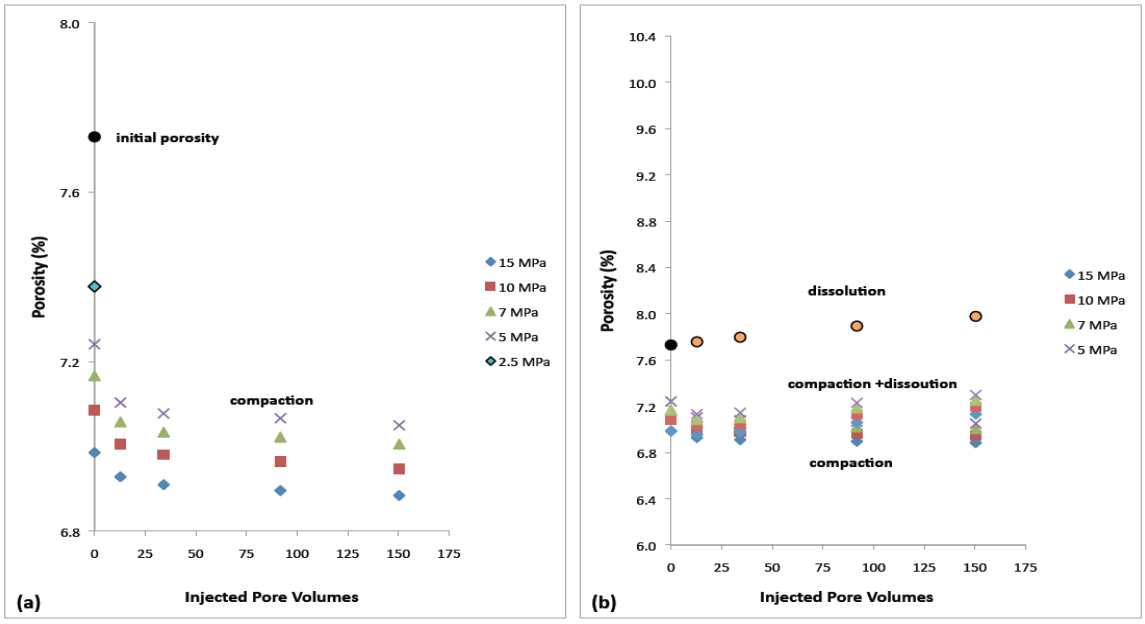

Figure 4: Variation of the porosity of the MSA tight limestone as a function of the injected pore volumes. The sample experiences a dissolution-driven compaction under the effect of the applied stress, eventualy leading to porosity change.

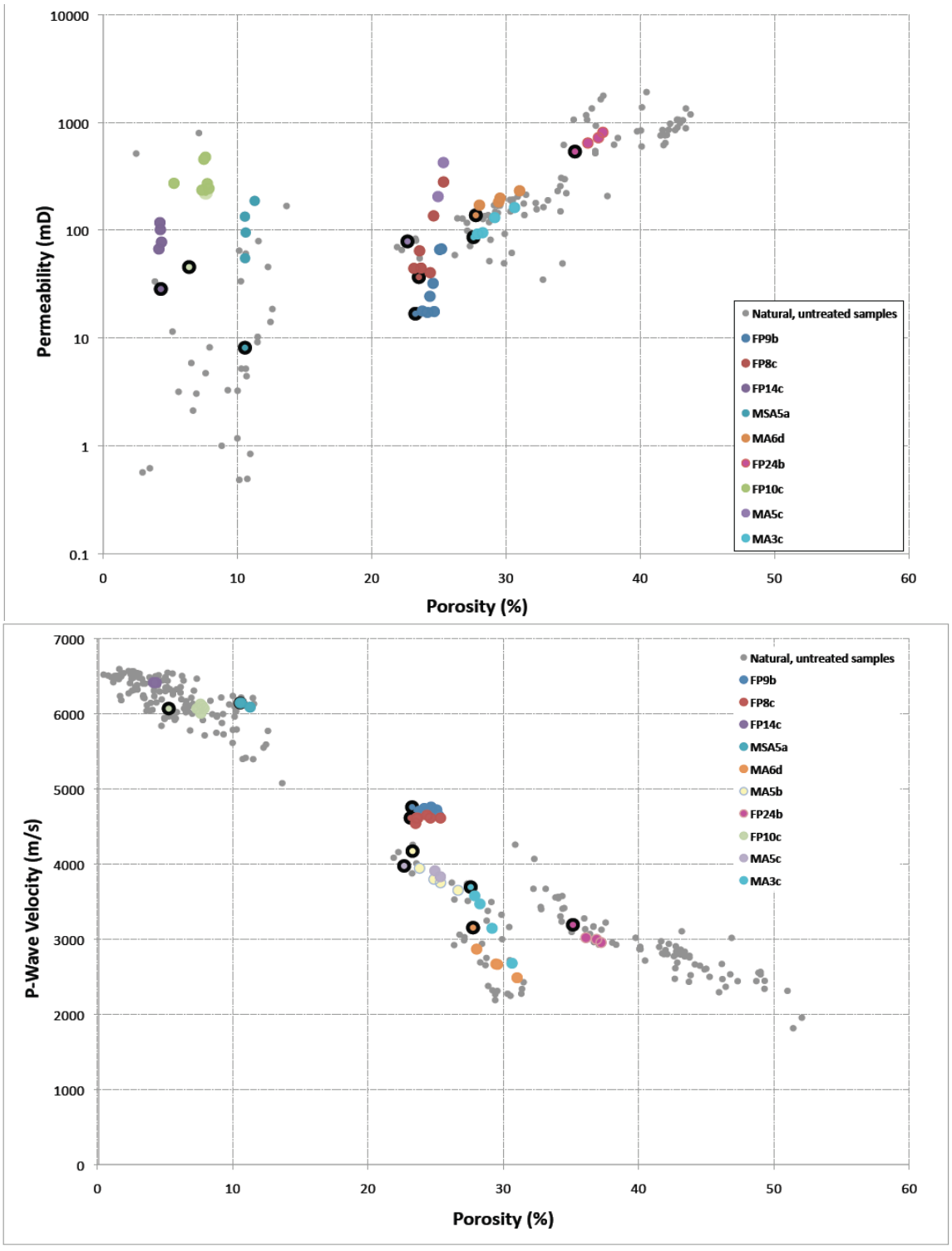

Figure 5: Evolution of P- and S-wave velocity (top) and permeability (bottom) of the injected sampls as functions of porosity. Data are compared to the natural diagenetic trends of untreated carbonate samples (gray circles). Data refer to dry samples measured after being injected.

Differentiating chemical effects and pressure effects on the elastic properties of the Lower Tuscaloosa sandstone in Cranfield, Mississippi by injecting carbon dioxide rich brine. (Corey Joy, The University of Texas at Austin, Tiziana Vanorio, Stanford Rock Physics Laboratory, and Mrinal K. Sen, The University of Texas at Austin. SEG Extended Abstract 2011)

Current and evolving regulatory and commercial environments governing injection may require monitoring. Rock physics can be used to determine the effect that these injected fluids have on the reservoirs with time. Performing rock physics experiments on site-specific core plugs can give one the ability to differentiate between chemical effects and pressure effects on the elastic properties of the rock while injecting a chemically reactive substance, or reactant. Detailed Area Study (DAS) of Cranfield, Mississippi, has been selected as a candidate for carbon dioxide enhanced oil recovery. This provides an opportunity to study the geochemical and geophysical effects of injecting carbon dioxide into the subsurface. Cranfield DAS is a unique site in that a variety of methods are used to monitor carbon dioxide in the subsurface. One of such methods is time-lapse seismic monitoring. The integration of rock physics with 4D seismic technology is an effective tool to quantitatively characterize the reservoir dynamics associated with fluid injection. Nevertheless, changes in seismic velocities are mostly interpreted as variations of physical parameters— such as saturation, pore fluid pressure, temperature, and stress. Hovorka (2009) reported that in the Frio Formation, dissolved CO2 lowered the pH of the brine, dissolving calcite from the matrix and large amounts of iron (Fe) and manganese (Mn) (Kharaka et al., 2006). Furthermore, laboratory investigation of CO_2-brine-rock interaction within samples from the Tuscaloosa sandstone formation at Cranfield, Mississippi reported a rapid increase of dissolved iron immediately after injection, caused by the dissolution of iron-bearing carbonate minerals and ironchlorite (Karamalidis et al., 2010). Therefore, it is essential to differentiate the effects on the elastic properties due to physical (i.e., pressure) and chemical processes occurring upon injection of carbon dioxide into the Lower Tuscaloosa formation.

Since chemical reactions depend on pressure, temperature and chemical components, it is important to simulate in-situ conditions as well as possible. Recreating the in-situ fluid is one of the most important steps in this experimental process, because the fluid in place may promote chemical dissolution/precipitation and/or buffer the injected reactant. At the Cranfield Detailed Area Study, the in-situ brine of the Tuscaloosa formation is Na-Ca-Cl type with about 152,000 milligrams per liter of total dissolved solids (Karamalidis et al., 2010). According to La Chatelier's principle, the presence of high calcium content in the brine may inhibit dissolution of calcite. The pH values of the synthetic Tuscaloosa brine and the CO_2 rich Tuscaloosa brine were 5.8 and 3.4 respectively. The temperature and pressure of the formation also control the chemical reactions.

Confining pressure plays an important role in simulating the chemical reactions. We use a pressure column approach to resolve the confining stress. According to well logs, the average density is roughly 2.1 grams per cubic centimeter (g/cc). The formation under consideration is roughly 3.2 kilometers (km) deep. Therefore, the confining stress is roughly 65 MPa. The pore pressure before injection is approximately 31 MPa; the pore pressure after injection is approximately 38 MPa (Hovorka et al. 2009). However, due to the limitations of the pressure vessel used, both confining and pore pressures are scaled back by 10 MPa in order to maintain in-situ differential pressure. Therefore, the confining pressure, initial pore pressure, and final pore pressure are 55 MPa, 21 MPa, and 28 MPa respectively. Note that the experiments are performed at room temperature in order to hold one variable constant. The characterization of the samples included Helium porosity, Klinkenberg-corrected nitrogen permeability, and ultrasonic P- and S-wave velocities. The plugs were jacketed with rubber tubing to isolate them from the confining pressure medium. PZT-crystals mounted on steel endplates generated P- and S-waves (1 MHz for P-waves and 0.7 MHz for S-waves). Three linear potentiometers were used to measure length changes of the samples as a function of stress. The length changes were related to changes in porosity by assuming that pore contraction was the main cause of strain. The accuracy in velocity measurements was estimated to be about ±1%. Compressional and shear wave velocities are measured at various confining pressures after multiple injections of carbon dioxide rich brine. The velocities are measured when the sample is dry to minimize dispersion. Measurements of a dry sample also show how the frame changes with each injection. Monitoring the changes in the elastic moduli of the dry frame as a function of injected volumes is also important for fluid substitution modeling (Vanorio et al., Geophysics in press, 2011). The first step in the experimental process is to prepare the sample and record a baseline of the mechanical properties. Since the sample is sandstone with some clay, the core plug was dried at 70ºC for 72 hours. The initial geometry and mass of the core plug were recorded to note any change in bulk properties after carbonic acid injection. The initial length, diameter and mass of the sample are 27.5 millimeters (mm), 25.3 mm, and 29.1 g respectively. The initial porosity of the sample is 21%. The initial permeability of the sample is 5 millidarcies (mD). After measuring porosity and permeability, the sample is inserted into the pressure vessel where it undergoes a series of loadings, reactant injections, and unloadings. Measuring the pressure dependency of P- and S- wave velocities for the dry core plug, before any injection, establishes a baseline for the elastic properties of the rock. Both the compressional and shear velocities of the core plug are measured as a function of confining pressure, in this case ranging from 0 to 55 MPa. Smaller pressure intervals are used at low confining pressures to map the nonlinear portion of the compaction curve. The following list is the workflow used in these experiments:

1. Load sample to 55 MPa.
2. Inject sample with carbon dioxide rich synthetic Tuscaloosa brine to a pore pressure of 28 MPa.
3. Measure change in length, Vp, and Vs.

4. Flush the sample with a given number of pore volumes of carbon dioxide rich synthetic Tuscaloosa brine while maintaining a pore pressure of 28 MPa.
5. Measure change in length, Vp, and Vs.
6. Leave saturated sample in current conditions for 12 hours.
7. Measure changes in length, Vp, and Vs.
8. Drain fluid and dry with gaseous helium at 150 psi for five hours. Now the pore pressure is zero.
9. Measure changes in length, Vp, and Vs while decreasing confining pressures to 20 MPa.
10. Repeat steps 1-9 to monitor the effect on Vp and Vs while increasing pore fluid volumes

Measuring velocity at various differential pressures after injection may simulate changing the pore pressure. Knowing the impact of pore pressure on the elastic properties of the core plug can enable one to resolve the change in velocity due to the chemical reaction and the change in velocity due to the change in pore pressure. However, loading and unloading a core plug in this manner may permanently deform the microstructure of the sample. In order to understand if the sample was experiencing any damage revealed by hysteresis, we performed an experimental test in which we loaded and unloaded a “twin” sample with the same stress path. The “twin” core plug comes from the depth as the injected sample and has the same porosity and permeability. SEM images of the top of the samples (i.e., injection side) are taken before and after the injection experiments to monitor changes in the rock’s microstructure. The fluid is regularly sampled at the outlet to measure pH and iron content using the titration method. We use a digital titrator (HACH LANGE 16900) and a commercial TitraVer 0.0716 M solution as titrant.

The compaction curves show that velocities increase with increasing confining pressure (Figure 6). As typically observed in sandstones, the compressional and shear wave velocities increase quickly with confining pressure up to 20 MPa. At a confining pressure of 20 MPa the curve flattens and is approximately linearly proportional to confining pressure. After the injection of the first 25 pore volumes, the P and S-wave velocities of the dry frame decreased by roughly 10%. Small changes in velocities are observed after subsequent carbonic acid injections. The compaction curves following injection behave similarly to the compaction curves pre-injection; from 20 to 55 MPa the velocity is linearly proportional to differential pressure (Figure 6).

The elastic moduli decrease after each injection. The largest decrease in elastic moduli is observed after the first injection. The bulk and shear moduli remain fairly constant after the second injection (Figures 7 and 8). Using the linearity of the compaction curves, we found the P and S-wave velocities at a differential pressure of 26 MPa, which is the current in-situ differential pressure of the injection site. After adjusting density for change in volume, the bulk and shear moduli were extracted from the velocities (Figures 9 and 10). The equations for the shear and bulk moduli as a function of injected pore volumes, Pv, are

$$\mu(Pv) = 11.722 + 0.7404 * \exp(-1.1316 * Pv)$$
$$K(Pv) = 16.713 + 2.2827 * \exp(-0.041093 * Pv)$$

After the final injection and drying in the oven for three days at 60ºC, the final length, diameter, and mass of the core plug are 27.3 mm, 25.3 mm, and 29.1 grams respectively. The final porosity and permeability are 20.2% and 10 mD respectively. The sample has hardly changed in the context of size, weight, and petrophysical properties. However, the elastic properties have greatly changed, which are a manifestation of change in microstructure. Microstructural changes are observed in the core plug after the injection of CO_2 rich brine (Figures 11 and 12). The sand grains are not affected by the reactant and do not compact. On the other hand, the pore filling material experiences significant deformation. Dissolution of the material under pressure occurs at grain contacts and induces cracks. The same stress path was applied to the "twin" as the injected sample. The compaction curves of the "twin" do not show change in P or S-wave velocities while loading and unloading within error.

The purpose of this paper is to study the effects of chemical reactions and pressure effects on the elastic properties of the Lower Tuscaloosa sandstone to better quantify the amount of carbon dioxide in the subsurface using seismic methods. The effects of changing the differential pressure did not have a large effect on the compressional and shear wave velocities for this rock. Decreasing the confining pressure from 33 to 26 MPa decreased P and S-wave velocities by roughly 60 and 20 m/s respectively.

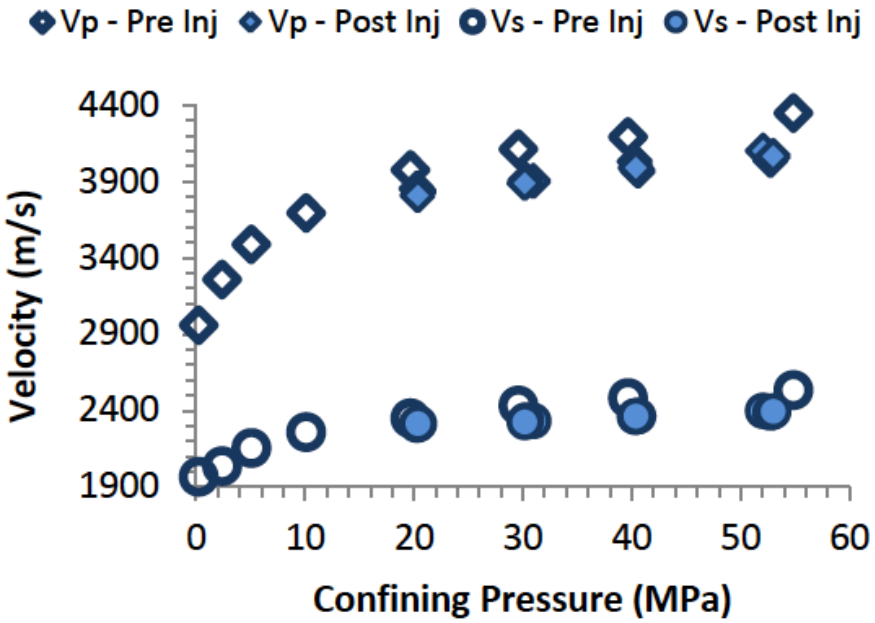

Figure 6: Compaction curves of the dried sample pre and post-injections. Pore pressure is zero.

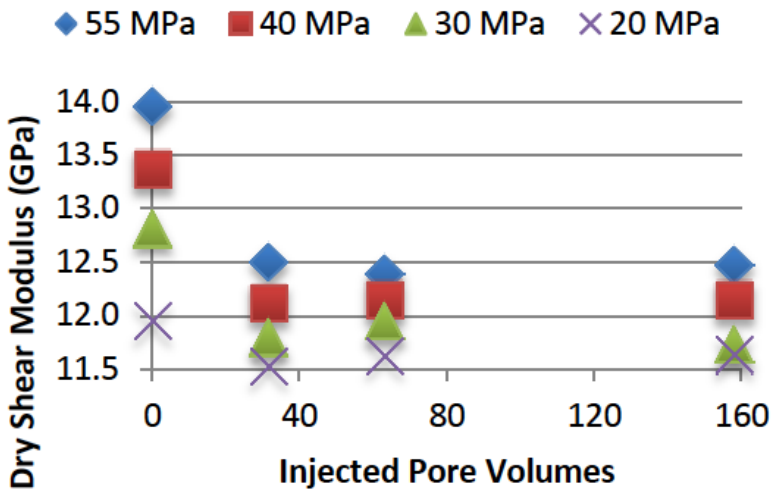

Figure 7: Shear modulus of the dry frame versus injected pore volumes colored by confining pressure.

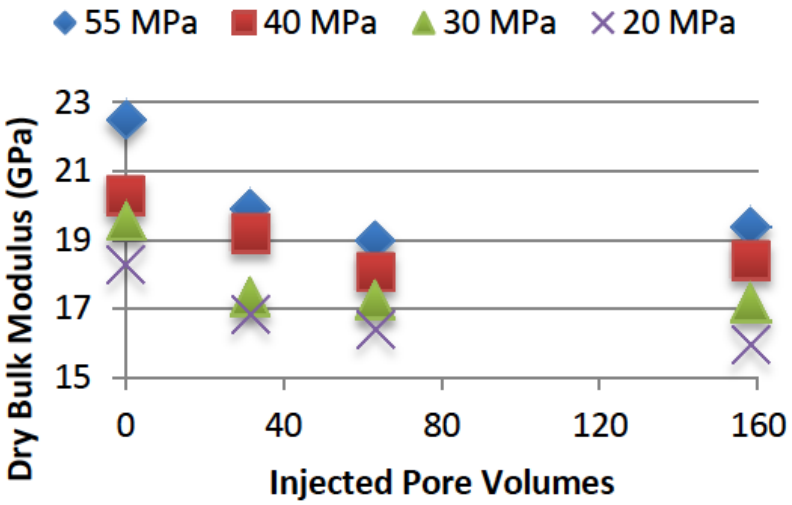

Figure 8: Bulk modulus of the dry frame versus injected pore volumes colored by confining pressure.

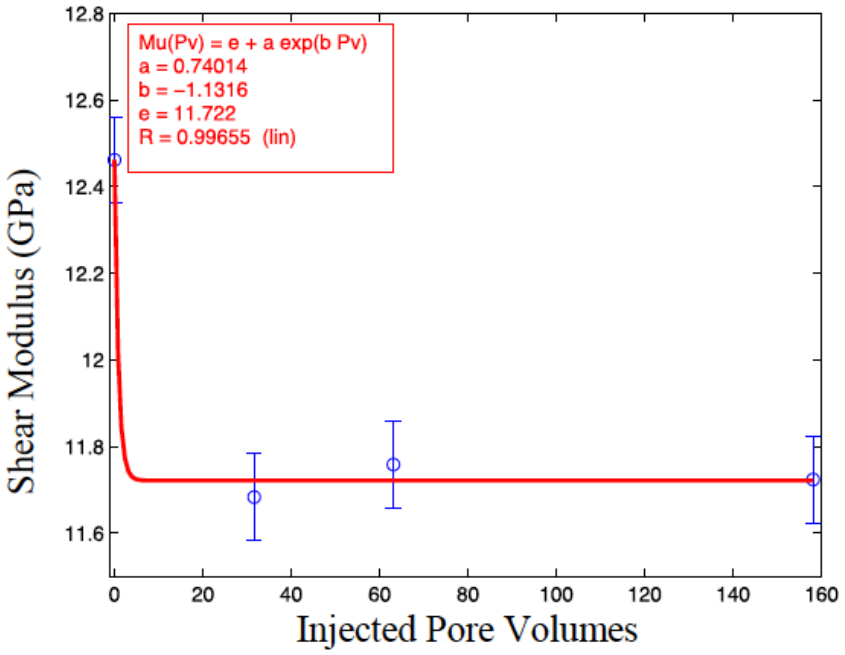

Figure 9: Shear modulus of the dry frame versus injected pore volumes for a differential pressure of 26 MPa.

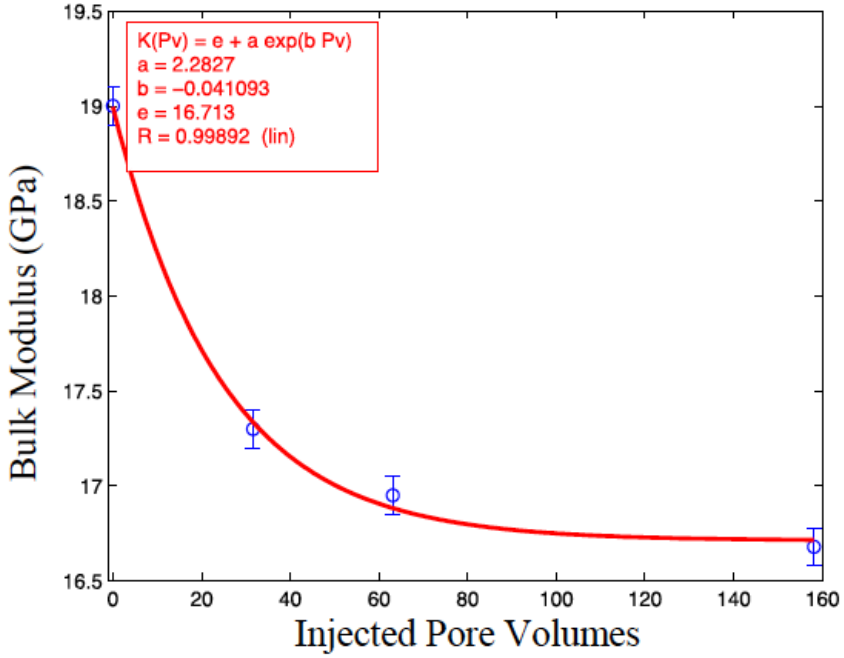

Figure 10: Bulk modulus of the ddry frame versus injected pore volumes for a differential pressure of 26 MPa.

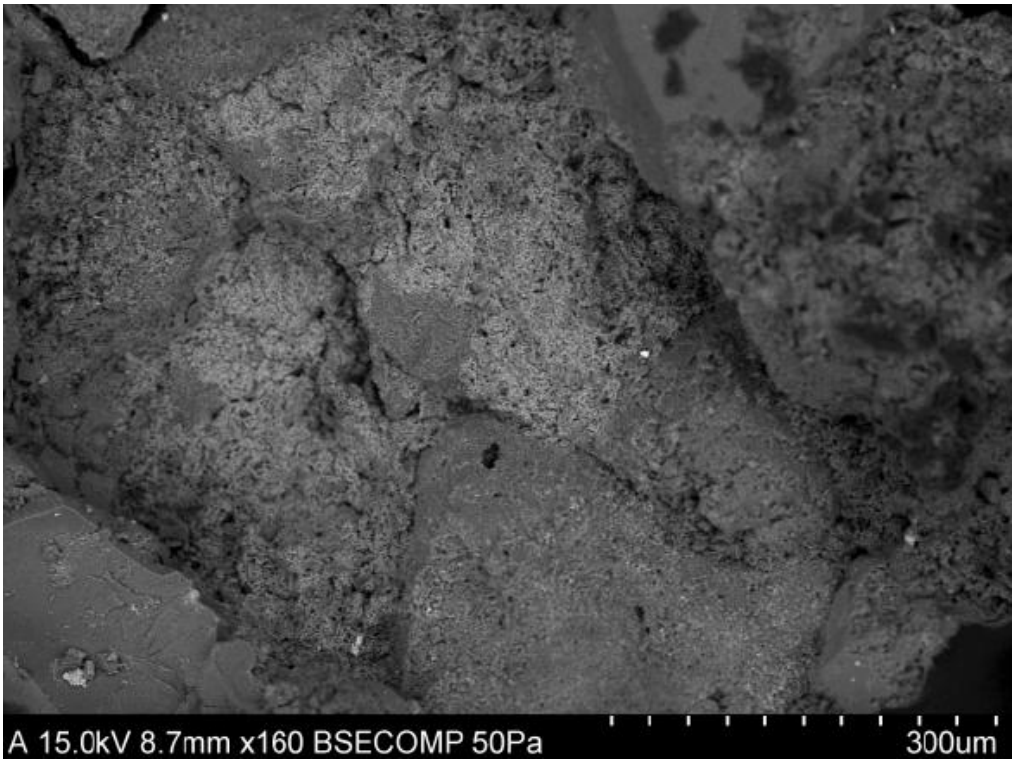

Figure 11: SEM image of the core plug before CO^2 rich brine.

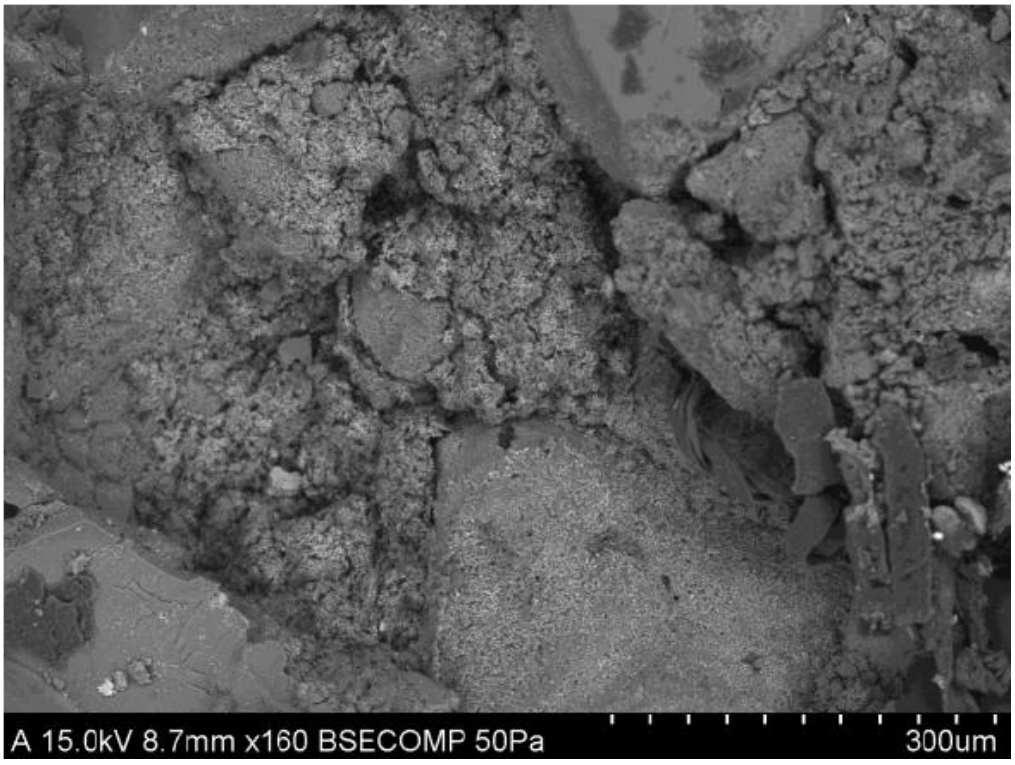

Figure 12: SEM image of the core plug after CO^2 rich brine.

Progress

Sequestration of CO_2 in geological formations is one of the carbon-management technologies having the potential to substantially reduce greenhouse gas emissions while achieving energy sustainability. To translate such potential into concrete development outcomes, realized benefits, and policy, common concerns (i.e. pore pressures reactivating faults or fractures, risk of leakages, and loss of storage capacity) need to be dispelled. These concerns are thus intimately associated with our ability to use geophysical techniques to monitor chemical processes and their effects on the rock properties. Exploring the links between geophysical observables, rock physical properties, and geochemical induced long-term changes upon CO_2 sequestration and introducing them into standard monitoring programs are necessary steps to go towards quantitative predictions of pore pressure, saturation, and storage capacity.

This project is on track to meet the overall objectives. The laboratory measurements for ultrasonic monitoring of rock changes associated with CO_2 injection have been completed. The team at Rice University is developing, via measurement and simulation, a modeling framework that can help to bridge the gap between laboratory and field geochemical observations.

Future Plans

The laboratory and modeling work at Rice University will continue until the project end. At Stanford, rock physics modeling will continue, aimed at providing a framework for understanding the seismic signatures of CO_2 saturation, as well as chemical changes to the rock frame.

References

1. Anselmetti, F.S. and Eberli, G.P., 1993, Controls on Sonic Velocity in Carbonates, Pageoph, vol. 141, pp. 287-323
2. Carman, P. C., 1961, L'écoulement des gaz á travers les milieux, 1961, Bibliothèque des Sciences et Techniques Nucléaires, Presses Universitaires de France, Paris.
3. Hovorka, S., 2009, Frio brine pilot: The first U. S. sequestration test: Southwest Hydrology, 8, no. 5, 26– 31.
4. Karamalidis, A., J. A. Hakala, C. Griffith, S. Hedges, and J. Lu, 2010, Laboratory investigation of CO2 — Rock-brine interactions using natural sandstone and brine samples from the SECARB Tuscaloosa injection zone: Geological Society of America Annual Meeting, Paper no. 86-10.
5. Kharaka, Y. K., D. R. Cole, S. D. Hovorka, W. D. Gunter, K. G. Knauss, and B. M. Freifeld, 2006, Gaswater- rock interactions in Frio formation following CO2 injection: Implications for the storage of greenhouse gases in sedimentary basins: Geology, 34, no. 7, 577–580, doi:10.1130/G22357.1.
6. Lu, J., Y. K. Kharaka, D. R. Cole, J. Horita, and S. Hovorka, 2009, Reservoir fluid and gas chemistry during CO2 injection at the Cranfield field, Mississippi, USA
7. Mavko, G. and Jizba, D., 1991, Estimating grain-scale fluid effects on velocity dispersion in rocks, Geophysics, 56, 1940-1949.
8. Mavko, G., Mukerji, T., and Dvorkin, J., 1998, The Rock Physics Handbook: Tools for Seismic Analysis in Porous Media, Cambridge University Press.
9. Scotellaro, C., T. Vanorio, and G. Mavko, 2008, The effect of mineral composition and pressure on carbonate rocks: 77th Annual International Meeting, SEG, Expanded Abstracts, 26, 1684–1689.

10. Vanorio T., and Mavko G., The Effect of Microstructure on the Acoustic Properties of Carbonate Rocks: Geophysics 76, 105-115
11. Vanorio, T., C. Scotellaro, and G. Mavko, 2008, The effect of chemical and physical processes on the acoustic properties of carbonate rocks: The Leading Edge, 27, 1040– 1048, doi:10.1190/1.2967558.
12. Weger, R. J., G. P. Eberli, G. T. Baechle, J.-L. Massaferro, and Y. F. Sun, 2009, Quantification of pore structure and its effect on sonic velocity and permeability in carbonates: AAPG Bulletin, v. 93, p. 1297–1317, doi:10.1306/05270909001.

Contacts

Gary Mavko: mavko@stanford.edu
Tiziana Vanorio: tvanorio@stanford.edu
Denys Grombacher: denysg@stanford.edu
Sally Benson: smbenson@stanford.edu
Stephanie Vialle: svialle@stanford.edu
Andreas Luttge: aluttge@rice.edu
Rolf Arvidson: rolf.s.arvidson@rice.edu
Corey Joy: corey.ajoy@gmail.com
Mrinal Sen: mrinal@ig.utexas.edu